World Academy of Science, Engineering and Technology
International Journal of Materials and Metallurgical Engineering
Vol:18, No:2, 2024

Application of Voltammetry to Study Corrosion of Steel Buried in Unsaturated Soil in the Presence of Cathodic Protection

Mandlenkosi George Robert Mahlobo, Peter Apata Olubambi, Philippe Refait

***Abstract*—**The aim of this study was to use voltammetry as a method to understand the behavior of steel in unsaturated soil in the presence of cathodic protection (CP). Three carbon steel coupons were buried in artificial soil wetted at 65-70% of saturation for 37 days. All three coupons were left at open circuit potential (OCP) for the first seven days in the unsaturated soil before CP which was only applied on two of the three coupons at the protection potential -0.8 V vs. Cu/$CuSO_4$ for the remaining 30 days of the experiment. Voltammetry was performed weekly on the coupon without CP while electrochemical impedance spectroscopy (EIS) was performed daily to monitor and correct the applied CP potential from ohmic drop. Voltammetry was finally performed the last day on the coupons under CP. All the voltammograms were modeled with mathematical equations in order to compute the electrochemical parameters and subsequently deduce the corrosion rate of the steel coupons. For the coupon without CP, the corrosion rate was determined at 300 µm/y. For the coupons under CP, the residual corrosion rate under CP was estimated at 12 µm/y while the corrosion rate of the coupons, after interruption of CP, was estimated at 25 µm/y. This showed that CP was efficient due to two effects: a direct effect, from the decreased potential, and an induced effect, associated with the increased interfacial pH that promoted the formation of a protective layer on the steel surface.

***Keywords*—**Carbon steel, cathodic protection, voltammetry, unsaturated soil, Raman spectroscopy.

I. Introduction

CARBON steel is widely used when large quantities of steel are needed due to its low market price and mechanical properties that are acceptable for many applications such as underground pipeline transportation [1]. There is for instance approximately 37 000 km of natural gas pipeline networks in France, 1 000 000 km in the world and 3 500 000 km of all fluids pipeline networks in the world. However, buried carbon steel has been reported to be very susceptible to corrosion when exposed to the soil environment [2]-[11]. Organic coatings together with CP are used to protect buried carbon steel from external corrosion. The criteria for pipeline protection against corrosion according to the EN 12954: 2001 standard specify reference values of the protection potentials to be applied depending on soil conditions. According to this standard, the CP is assumed to be efficient when the residual corrosion rate is lower or equal to 10 µm/y. However, the relationship between the polarization level, i.e., the applied protection potential, and the residual corrosion rate is still questionable and may depend on soil parameters such as composition, moisture content.

CP effectiveness to protect buried carbon steel pipelines has been extensively studied to understand its failure mechanism under various soil conditions [4], [5]. Various factors have been reported to be the fundamental influence towards the CP effectiveness. These factors include primarily those affecting the transport of crucial components (O_2, OH^-, etc.) such as the defect size and properties of the environment surrounding the protected object [4], [5]. The decline in CP effectiveness implies that corrosion of buried carbon steel pipeline prevailed and could lead to more pipeline failure if not studied. Corrosion in soils is a multiscale process: at its core is the electrochemical process at the metal surface, which is highly influenced by film/droplet formation on the metal, the geometry and liquid phase chemistry of such films as well as the development of oxide layers on the metal surface [6]. Soil moisture is generally considered as the most influent parameter because it strongly affects the most crucial point, the transport of O_2 from the atmosphere to the steel surface [6], [7]. This has turned the focus into monitoring and surveying the CP system by determining the residual corrosion rate of the buried carbon steel under all soil properties which will, in turn, quantify the CP effectiveness. It was demonstrated that the in unsaturated soils (about 35%-65% saturation) CP led to an increase of the active area of the metal linked to electro-capillarity effects [8]. The research carried out by Barbalat et al. [9], [10] developed a method to estimate the actual residual corrosion rate of carbon steel under soil in the presence of CP. This method was based on voltammetry. The idea was to model the polarization curve with kinetic laws to obtain the expression of the anodic current density as a function of potential.

The aim of this study was to use voltammetry to quantify CP efficiency by comparing the behavior of carbon steel coupons buried for 37 days in unsaturated soil (65-70% saturation) with or without CP. The voltammograms obtained were mathematically modeled to compute some of the electrochemical data and subsequently deduce steel corrosion rate. The characterization of the corrosion products was achieved by Raman spectroscopy at the end of the

Mandlenkosi, G.R. Mahlobo is with Department of Chemical Engineering, University of South Africa (e-mail: mahlomg@unisa.ac.za).

Peter, A. Olubambi is with Center for Nanoengineering and Advanced Materials (CeNAM), University of Johannesburg, Johannesburg, 2028, South Africa.

Philippe Refait is with Laboratoire des Sciences de l'Ingénieur Pour l'Environnement (LaSIE) - UMR 7356, University of La Rochelle/CNRS, La Rochelle, France.

experiments.

II. Experimental Procedure

A. Preparation of Steel Coupons

Carbon steel S235JR with the nominal composition 0.097 C, 0.49 Mn, 0.02 P, 0.09 Si, 0.05 Cr, 0.11 Ni, 0.16 Cu, 0.042 S (wt%) and balance Fe was chosen for the test coupons. Cylindrical coupons of diameter 30 mm and 2 mm thickness were cut from the same carbon steel rod, connected to a copper wire and embedded in epoxy cold resin. The coupons were prepared through grinding and polishing on 80 to 600 grits. After grinding, the coupons were thoroughly rinsed with Milli-Q water and dried. Only one circular face of the coupon (with an area of 7.07 cm^2) was exposed to the environment.

B. Soil Preparation and Electrochemical Cell Set-Up

This study made use of an artificial soil composed of 83 wt% fine sand particles (SiO_2, average particle size 22 µm), 14.5 wt% clay (kaolinite) and 2.5 wt% peat. The soil moisture content was set at an initial value of 70% saturation using the electrolyte solution prepared as shown in Table I at room temperature (19-25 ºC). It was observed in a previous study that soil moisture tended to decrease slightly even with the cell hermetically sealed as part of the water evaporated into the air layer trapped above the soil in the cell [7]. It was estimated from previous results [7] that after some time, the soil reached a moisture level about 65% saturation.

TABLE I
Chemical Composition of the Electrolyte Solution

Comp.	NaCl	$CaCl_2 \cdot 2H_2O$	$MgCl_2 \cdot 6H_2O$	$Na_2SO \cdot 7H_2O$	$NaHCO_3$
Conc. (g/l)	0.584	0.294	0.203	0.402	0.168

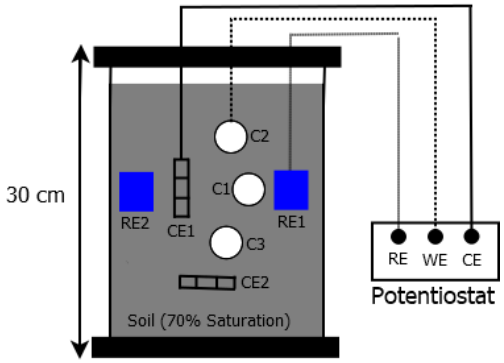

Fig. 1 Schematic representations of electrochemical cell for corrosion studies in the soil

A 25 cm × 30 cm plexiglass cell, identical to that designed for previous work [7], was used to bury three coupons at the same depth inside the unsaturated soil ensuring that they were as far apart from each other as possible. The soil was filled up to about 5-10 cm below the top of the cell to allow the remaining space for air into the system. Care was taken to not to compact the soil inside the cell in order to create enough space (micropores) for the movement of the electrolyte. However, the cell was closed with a lid to avoid excess drying of the soil. The prepared carbon steel coupons were used as working electrodes. The reference electrodes were the Celco 5 (COREXCO) $Cu/CuSO_4$ electrodes (+0.316 V/SHE at 25 ºC) specifically designed for soil experiments, commonly used in the field and also used in previous studies [7], [8], [11]. All electrochemical potentials in this study were expressed with reference to this electrode, i.e., V vs. $Cu/CuSO_4$. Two titanium grids placed at vertical and horizontal orientation with respect to the steel coupons inside the cell were used as counter electrodes. Probes were also inserted in the electrochemical cell to monitor the soil moisture content and O_2 concentration.

C. Experiments in Unsaturated Soil Environment

Three carbon steel coupons were buried in the prepared 65-70% saturated soil for 37 days according to the set-up shown in Fig. 1. The coupons were subjected to OCP environment for the first seven days of the experiment. After the first 7 days of the experiment at OCP, CP was applied but only on two of the three coupons for the remainder of the experiment, while electrochemical measurements were performed on the third coupon weekly. The two coupons under CP were denoted as CP1 and CP2 while the coupon left at OCP for the entire experiment was denoted as WE.

D. Electrochemical Studies

All electrochemical measurements were performed in the cell shown in Fig. 1 using a GAMRY Interface 1000 potentiostat monitored by the Framework V4.35 software. First, OCP measurements were performed for each of the three buried coupons during the first 7 days of the 37 days of the experiment. Results were analyzed with the GAMRY Echem Analyst software. EIS was used to determine the electrical resistance of the soil (R_s) between the reference electrode and each of the three coupons set in the cell. The frequency was varied between 10 kHz and 200 MHz and the AC voltage perturbation amplitude (peak to peak) was 0.03 V around the applied protection potential of the sample. This high amplitude was required because of the important ohmic drop due to soil resistivity. The linearity of the system was checked by varying the amplitude of the AC signal applied to the sample. The R_s corresponds to the real part of the impedance when the frequency tends towards infinity. It must be noted that R_s is mainly linked, in unsaturated soils, to the active area of the electrode [7], [8], [11], i.e., the area really in contact with the electrolyte present in the pores of the soil. More precisely, R_s is inversely proportional to the active area. For instance, if the soil dries, i.e., the amount of electrolyte present in the pores decreases, then the active area decreases and R_s increases. The value of R_s then indicates whether soil moisture varies in the vicinity of the coupon.

Voltammetry around OCP (VAOCP) [7], [12] was applied at a scan rate of 0.1 mV/s in order to determine the corrosion rate (τ_{cor}) at seven-day time intervals. The polarization curve during the VAOCP measurements was recorded from the OCP up to an applied potential E_{on} = OCP+0.08 V and then down to E_{on} = OCP-0.08 V. However, due to the large ohmic drop (next section), the variations of E_{Free} were much smaller, i.e., $\Delta E_{Free} \sim \pm$ 0.03 V instead of the expected range of ± 0.08 V.

On the last day of the experiment, i.e., day 37, the VAOCP potential range was then extended from OCP ± 0.08 V to OCP ± 0.2 V. The voltammograms obtained were mathematically modeled by the Origin Lab 9.0 Software, following the methodology thoroughly described elsewhere [7], [12]. Mathematical models based on theoretical kinetic laws were used to compute the relevant electrochemical parameters and consequently deduce the corrosion rate $\tau_{cor,}$ from the corrosion current density using Faraday's law.

E. Cathodic Protection

After the first 7 days at OCP, CP was applied only on two of the three coupons, i.e., CP1 and CP2, at the desired potential E_{CP} = -0.8 V vs $Cu/CuSO_4$ after correction of the ohmic drop. EIS measurements were performed at 12-hour time intervals to determine the electrical resistance of the soil electrolyte (R_s) between the reference electrode and each of the buried steel coupons. The applied potential was then corrected from ohmic drop according to (1):

$$E_{Free} = E_{on} - R_s \times j \quad (1)$$

where E_{Free} = corrected potential in V, E_{on} = applied potential in V, R_s = soil resistance in $\Omega.cm^2$ and j = current flowing through the electrode in A/cm^2. Since j may vary with time, E_{CP} may also vary until another correction is made (next day). It actually remained between -0.85 and -0.8 V vs $Cu/CuSO_4$. On day 7, just before CP was applied, a VAOCP experiment was performed on coupons CP1 and CP2 using the procedure described above for coupon WE. At the end of the experiment (day 37), polarization curves were acquired for both coupons CP1 and CP2. The curve was acquired in the positive-direction from the applied protection potential E_{CP} (~-0.83 V vs $Cu/CuSO_4$) up to E_{Free} (1) = -0.77 V vs $Cu/CuSO_4$ and then in the negative-direction direction down to E_{Free} (2) = -0.84 V vs $Cu/CuSO_4$. The positive and negative direction scans were mathematically modeled separately, using the Origin Lab 9.0 Software, according to the method developed previously [8]. This method was similar to that used for VAOCP [7], [12].

F. Raman Spectroscopy Analysis

Raman analysis was performed on a Jobin Yvon High Resolution Raman spectrometer (LabRAM HR Evolution) equipped with a confocal microscope, a Peltier-based cooled charge coupled device (CCD) detector and a solid-state diode pumped green laser (532 nm). The laser power was reduced between 25% and 1% of the maximum (i.e., between 1.94 and 0.07 mW) because excessive heating can induce the transformation of the analyzed Fe compounds into hematite α-Fe_2O_3. Spectra were recorded with the LabSpec software with a variable acquisition time which did not exceed 2 minutes.

III. Results

A. Electrochemical Measurements

1. Electrochemical Impedance Spectroscopy

Fig. 2 (a) shows, as an example, the EIS Nyquist diagrams obtained after 7, days 28 days and 37 days of the experiment for coupon WE. The EIS Nyquist diagram obtained after 7 days showed single semicircle capacitive loop at low frequencies indicating that the corrosion process on the steel surface was mainly controlled by charge transfer kinetics. This was the case for all three coupons as CP had not yet been applied at this stage. Furthermore, the EIS measurements performed afterwards showed a similar behavior even for the coupons under CP throughout the experiment until day 28 (Fig. 2 (a)), where the semicircle capacitive loop, observed earlier at day 7, appeared to have evolved into a large semi-circle with a high frequency behavior forming a straight line at an angle 45° with the real part of the impedance (Re (Z)). This behavior indicated that the corrosion process on the steel/ electrolyte interface was controlled by finite diffusion (of dissolved oxygen). Therefore, the information given by the EIS Nyquist data suggested that the corrosion process of the steel was controlled by charge transfer kinetics at the beginning but gradually changed into diffusion control at longer exposure times in soil (observed at day 28 in this study).

Figs. 2 (b) and (c) show the change of R_s with time for the coupons left at OCP (WE) and at CP (CP1 and CP2) respectively. The coupon WE showed declining R_s from day 1 to day 21. R_s increased slightly afterwards. The initial decrease of R_s could correspond to an increase of the active area. As the soil was not initially compacted, it could have settled naturally due to its own weight during the first 20 days, decreasing the size of the pores. This would explain the change of the EIS Nyquist diagrams. Initially, large gaps filled with air were present in the soil in the vicinity of coupon WE which facilitated the transport of O_2. As the pore volume decreased, air was expelled from the soil and thus allowed more electrolyte to occupy the soil pores. The transport of O_2 then became more difficult as it involved diffusion in the liquid phase and the corrosion process was then controlled by diffusion.

In contrast, the coupons under CP showed an increase in R_s from day 1 to day 7 (CP2) or 12 (CP1). This may have indicated that the soil in the vicinity of these coupons was drying, as observed previously [7]. For CP2, R_s decreased regularly after the first 7 days before stabilizing towards the end of the experiment. The variations of R_s observed for CP2 are consistent with those previously observed for coupons under CP [8]. Due to electrocapillary effects, a negative shift of the potential of a metal partially immersed in electrolyte usually leads to a decrease of the solid–liquid contact angle [8]. The liquid tended to spread on the surface when CP was applied so that the active area increased and R_s decreased. For CP1, the change of R_s was more complex. When CP was applied at day 7, the increase of R_s was slowed down as the application of CP induced effects associated with the formation of a protective layer on the steel surface [8]-[10]. Finally, R_s decreased until day 17 when a sharp increase of R_s occurred.

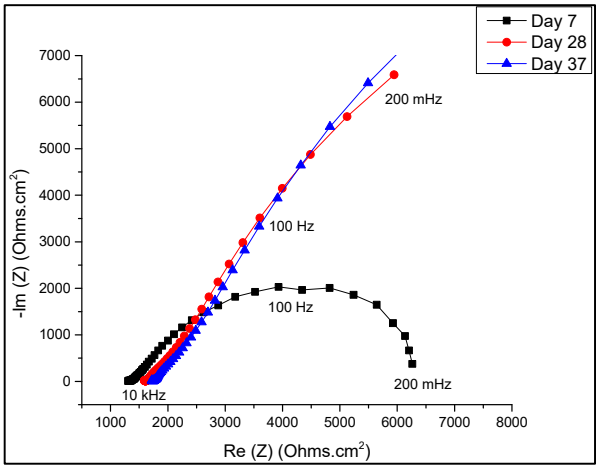

(a)

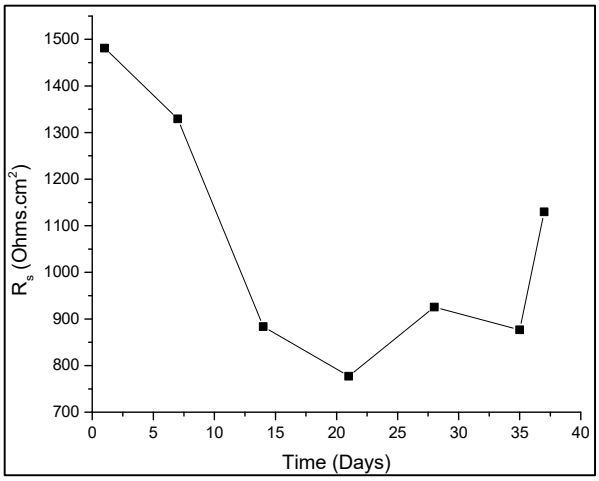

(b)

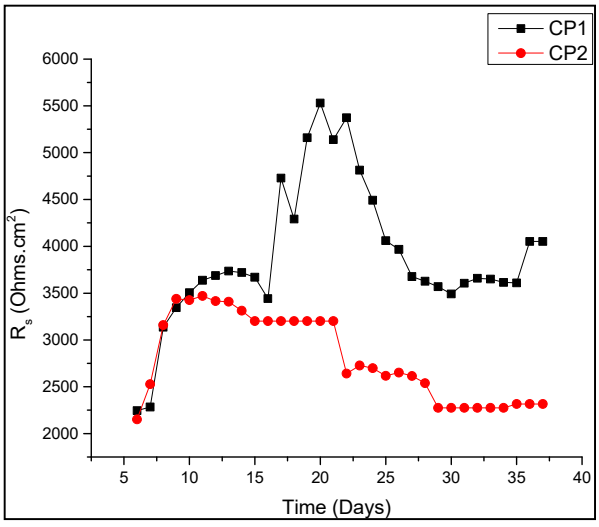

(c)

Fig. 2 (a) EIS Nyquist diagrams for coupon WE after 7, 28 and 37 days and R_s evolution with time for coupons: (b) WE and (c) CP1 and CP2

At day 22, R_s decreased again to reach values similar to those observed at day 17. These fluctuations of R_s indicated that the soil around coupon CP1 tended to dry naturally, through exchanges with the atmosphere lying above the soil, and conversely, CP tended to attract water towards the steel surface. Despite the same set-up being used to bury all three coupons for 37 days, it appeared that each coupon behaved differently due to active area which depended on the moisture content in the vicinity of each coupon.

2. Voltammetry

The voltammograms obtained from the experiments performed weekly on coupon WE are presented in Fig. 3. The corrosion potential (E_{cor}) of the steel at OCP was read directly from the voltammograms in Fig. 3 and appeared to decrease from the initial value (at day 7) of -0.73 to -0.81 V vs $Cu/CuSO_4$ (day 37). This decrease of OCP is consistent with an evolution from aerated to deaerated medium as proposed from EIS analysis. In order to fully understand the electrochemical behavior of the coupon, the voltammograms were modeled with theoretical and mathematical equations. This also allowed the estimation of the corrosion rate τ_{cor}.

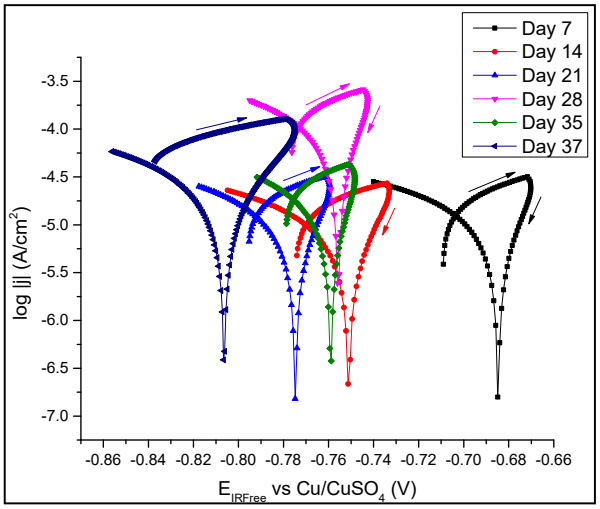

Fig. 3 Voltammograms for coupon WE buried in 65-70% saturated soil for 37 days

If the anodic region on the steel surface is controlled by the charge transfer kinetics, then the mathematical expression for the overall current density can be derived from the Butler-Volmer equation as follows [7], [8], [12]:

$$j(E) = j_a + j_{c,O2} = j_{cor}\left[e^{\beta_a(E-E_{cor})} - e^{\beta_{c,O2}(E-E_{cor})}\right] \quad (2)$$

where j(E) = overall current density in A/cm^2, j_a and $j_{c,O2}$ = anodic and cathodic (O_2 reduction in this case) current densities respectively in A/cm^2, j_{cor} = corrosion current density in A/cm^2, β_a and $\beta_{c,O2}$ = Tafel anodic and cathodic (O_2 reduction) coefficients respectively in V^{-1} and E_{cor} is the corrosion potential in V.

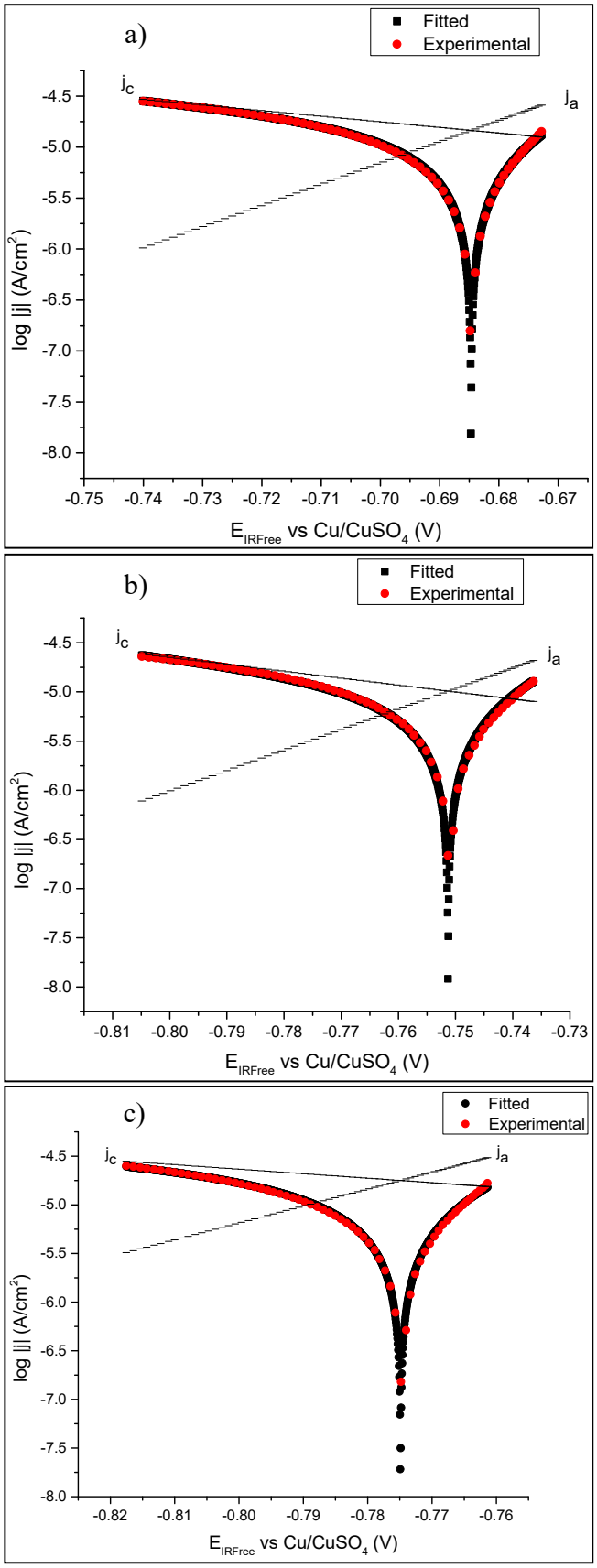

Fig. 4 Fitted voltammograms of coupon WE buried in 65-70% saturated soil after a) 7 days, b) 14 days, c) 21 days

Recalling the results obtained from EIS in the previous section, the corrosion process on coupon WE steel surface from day 7 to day 27 was characterized by the charge transfer kinetics and therefore (2) was used to model the voltammograms obtained from day 7 to day 21. Fig. 4 shows the voltammograms modeled using (2) for coupon WE on days 7-21. The electrochemical parameters computed from the mathematical modeling are shown in Table III, where R^2 during the modeling was higher than 0.999 with an error of ± 7%.

For days 28-37, the EIS Nyquist diagrams discussed in the previous section suggested that the process was controlled by diffusion. However, the voltammograms could be adequately fitted using (2), as displayed in Fig. 5. The influence of diffusion may have been too small to be detected by the VAOCP method.

The computed corrosion current densities, j_{cor}, were used to deduce the steel corrosion rate, τ_{cor}, using Faraday's law at each time of the experiment and are presented in Table II, together with the electrochemical parameters, namely β_a, $\beta_{c,O2}$ and R_s (determined by EIS). The anodic Tafel coefficient, β_a, was found at a constant value of 40 V^{-1}, while the Tafel cathodic coefficient, $\beta_{c,O2}$, varied from -8 to -30 V^{-1}. The τ_{cor} values deduced from the corrosion current density varied between 250 and 770 µm/y without any significant trend (Table II). This was attributed to the reliability of the VAOCP method. The voltammograms obtained from day 7 to day 35 were restricted to the scan range at about $\Delta E_{Free} \sim \pm 0.030$ V due to ohmic drop. This scan range was too small for VAOCP to be accurate and so the corrosion rate at OCP environment could only be concluded from the experiments performed at higher scan rates. The potential scan range was increased for the last experiment at day 37, leading to $\Delta E_{Free} \sim \pm 0.040$ V shown in Fig. 5 (c). The value obtained for τ_{cor} at day 37, i.e., 300 µm/y, was then more reliable and consistent with what was found in a previous study [7]. This corrosion rate was high, which confirmed that the soil remained aerated in the vicinity of coupon WE and was retained as the steel corrosion rate at OCP environment between day 7 and day 37.

TABLE II
ELECTROCHEMICAL DATA OBTAINED FROM MATHEMATICAL MODELING FOR COUPON WE

Days	E_{cor} (V vs Cu/CuSO$_4$)	j_{cor} (A/cm^2)	β_a (V^{-1})	β_c (V^{-1})	τ_{cor} (µm/y)
7	-0.73	2.12×10^{-5}	40	-8	250
14	-0.64	4.13×10^{-5}	40	-12	480
21	-0.64	6.57×10^{-5}	40	-10	770
28	-0.63	4.71×10^{-5}	40	-26	550
35	-0.59	4.71×10^{-5}	40	-30	550
37	-0.81	2.54×10^{-5}	40	-19	300

Similar values of ~300 µm/y were observed for soil moistures around 65% saturation and corresponded to a maximum, in agreement with previous results [8]. The highest corrosion rates corresponded to moisture levels of 60-65% saturation [6], [7], [11], [13]. In this case, most of the steel surface was in contact with the electrolyte but the pores were

sufficiently empty of liquid so that O_2 could be mainly transported without interference of the liquid [14].

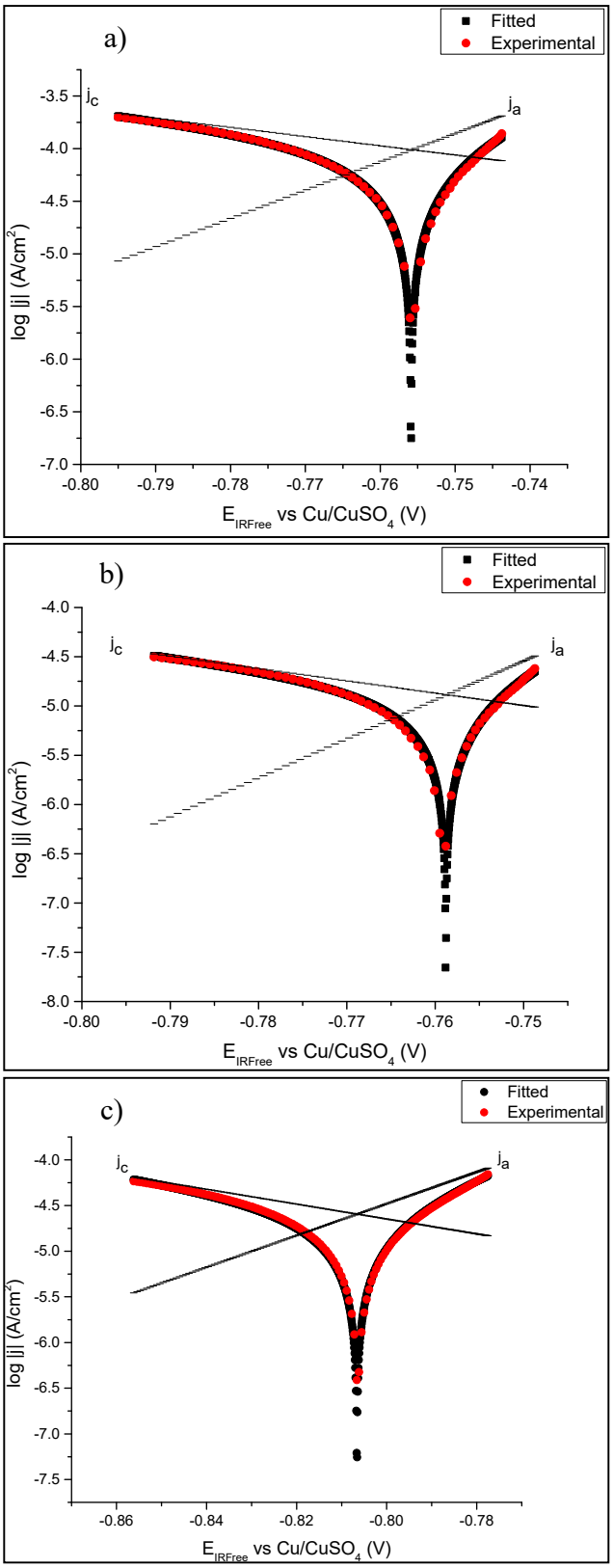

Fig. 5 Fitted voltammograms of coupon WE buried in 70% saturated soil after a) 28 days, b) 35 days, c) 37 days

3. Cathodic Protection

The VAOCP experiment performed at day 7 on the coupons CP1 and CP2 led to corrosion rates lower than for coupon WE. The results obtained for coupon CP2 are given in Table III. The corrosion rate at OCP was estimated at 160 µm/y for this coupon, while the value retained for coupon WE is twice as much (300 µm/y). This indicates that the soil in the vicinity of coupon CP2 differed differently from the soil in the vicinity of coupon WE. This seems to be common in unsaturated soil [7], [8], [11], because soil moisture is not homogeneous. This difference was also illustrated by the EIS data. For instance, at day 7, the R_s values for coupons WE and CP2 were about 1300 Ω cm^2 and 2600 Ω cm^2, respectively (Fig. 2), i.e., R_s (CP2) was twice as much R_s (WE). As the R_s value was inversely proportional to the active area, the active area of coupon CP2 was half that of WE at that time, most likely because the soil was drier. In unsaturated soils, the corrosion rate was mainly linked to the active area [7]. The results obtained here also illustrated this, as the corrosion rate of CP2 was half that of coupon WE.

The voltammogram obtained for coupon CP2 at day 37 is presented in Fig. 6 (and the computed electrochemical data in Table III). The overall experimental curve is shown in Fig. 6 (a). It could clearly be seen that the forward and reverse scans were different. In particular, the corrosion potentials were different, that measured on the positive direction, i.e., -0.825 V vs Cu/CuSO$_4$, being lower than that measured on the negative-direction, i.e., -0.775 V vs Cu/CuSO$_4$. This phenomenon may be due to the fact that CP, by increasing the cathodic reaction rate, consumed O_2. This explained why the first E_{cor} value was low. As the potential was gradually increased, the cathodic reaction was slowed down and the O_2 concentration in the steel/soil interface increased. When the scan was reversed, the environment had been slightly enriched in O_2, so that the rate of the cathodic reaction and the corrosion potential were higher.

TABLE III
ELECTROCHEMICAL DATA OBTAINED FROM MATHEMATICAL MODELING FOR COUPON CP2

R_s (Ω cm^2)	E_{cor} (V vs Cu/CuSO$_4$)	β_a (V^{-1})	$\beta_{c,O2}$ (V^{-1})	j_{cor} (A/cm^2)	τ_{cor} (µm/y)
Day 7, before CP was applied					
2528	-0.68	40	-10	1.35×10^{-5}	160
Day 37: Negative-direction scan					
2317	-0.775	(74)	-11	2.10×10^{-6}	25
Day 37: Positive-direction scan					
R_s (Ωcm^2)	E_{corr} (V vs Cu/CuSO$_4$)	β_a (V^{-1})	$\beta_{c,O2}$ (V^{-1})	$j_a(E_{CP})$ (A/cm^2)	τ_{rc} (µm/y)
2317	-0.825	17	(114)	1.11×10^{-6}	12

Both parts of the voltammogram, i.e., the positive-direction and the negative-direction scans were modeled separately. It was assumed that the predominant cathodic reaction was oxygen reduction as for the coupons at OCP, i.e., the possible influence of water reduction was not taken into account. Consequently, (2) was used again. Satisfactory results were obtained and the computed curves are compared to the experimental ones in Figs. 6 (b) and (c). Since the positive-

direction scan involved a very small cathodic region ($E < E_{cor}$), the value obtained for $\beta_{c,O2}$ was questionable and so is indicated in brackets in Table III. The same applies for the value of β_a obtained for the negative-going scan which involved a very small anodic region.

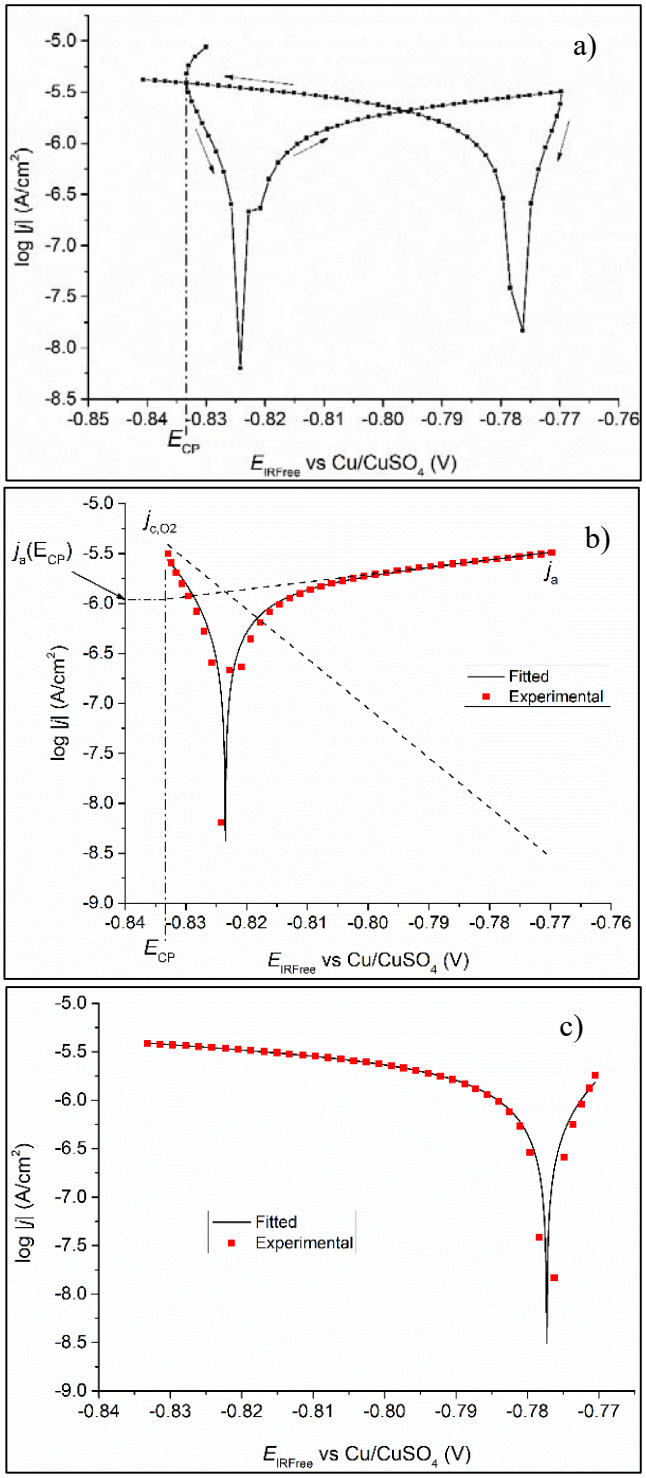

Fig. 6 Voltammograms obtained for coupon CP2 buried at day 37: a) complete experimental curve, b) positive-direction scan fitted with mathematical modeling and c) negative-direction scan fitted with mathematical modeling

The residual corrosion rate τ_{rc} of coupon CP2 was estimated from the positive-direction scan acquired from the applied potential E_{CP} up to -0.77 V vs $Cu/CuSO_4$. It was computed, using Faraday's law, from the value of the anodic current density j_a at the applied potential E_{CP}, as reported in Fig. 6 (b). The obtained value was τ_{rc} = 12 µm/y, similar to the expected order of magnitude (10 µm/y). The recommended protection potential is -0.85 V vs $Cu/CuSO_4$ according to the EN 12954: 2001 standard, i.e., a value slightly lower than that used in the present study. Consequently, it can be concluded that the recommended protection potential would have been sufficient to reach a residual corrosion rate lower than the expected value of τ_{rc} = 10 µm/y. The second part of the voltammogram, i.e., the negative-direction scan, was used to estimate the corrosion rate of coupon CP2 when CP was interrupted. The obtained corrosion rate was 25 µm/y, a value significantly lower than that measured for the same coupon at day 7, i.e., 160 µm/y. This showed that the application of CP for seven days promoted the formation of a protective layer on the coupon. In principle, CP increases the pH at the steel/electrolyte vicinity and if there is sufficient amount of Ca^{2+} and CO_3^{-} in the soil electrolyte, then the steel surface will exhibit calcareous deposit as a result of the precipitation of Ca^{2+} ions with carbonate ions on the steel surface [8]-[10]. The calcareous deposit may have a protective role. However, the increase of the interfacial pH can also promote the formation of a protective oxide layer [15].

The two effects of CP can then be quantified. The first effect was a direct effect that results from the decrease of the potential. When the potential was decreased from -0.775 V vs. $Cu/CuSO_4$ (E_{cor} of the negative-direction scan) to -0.834 V vs. $Cu/CuSO_4$ (E_{CP}, start of the positive-direction scan), the corrosion rate was reduced from 25 µm/y to 12 µm/y. The second effect was the indirect effect induced by CP, i.e., the formation of a protective layer due to the increase of the interfacial pH. This effect was responsible for the decreased τ_{cor} from 160 µm/y to 25 µm/y between day 7 and day 37.

B. Characterization

In order to comprehensively understand the characteristics of the steel/electrolyte interface, the characterization was performed first on the steel surface and on the portion of the soil attached to the entire surface area of the coupon. This was due to the black and brown colors observed when removing the soil from the coupon WE and it was believed that some of the corrosion products may have been detached from the surface of the coupon to the soil.

Fig. 7 shows typical Raman spectra obtained for the soil portion removed from the coupon WE (spectrum a) and for coupon CP1 surface (spectrum b). Spectrum a) is typical of goethite (α-FeOOH) [16], which was the only identified corrosion product on the soil recovered from the coupon surface and was an orange/brownish layer on the soil portion. This confirmed that goethite as the corrosion product detached from the coupon surface and adhered to the soil during the experiment. The formation of goethite requires O_2, which confirmed that the coupon was in contact with an aerated

environment.

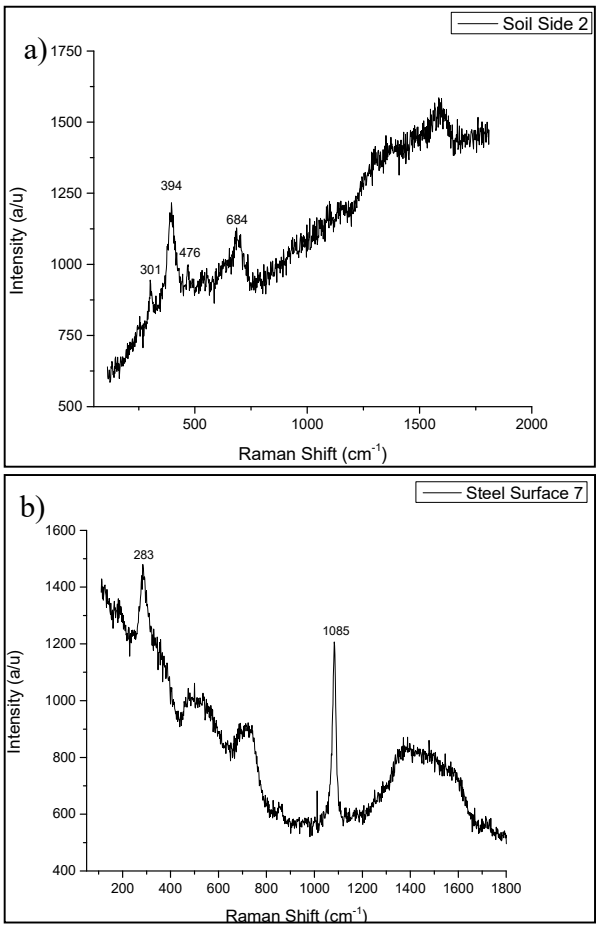

Fig. 7 Raman spectra obtained for: a) soil portion covering coupon WE surface area and b) coupon CP1 surface

In the presence of CP (coupon CP1) calcite ($CaCO_3$) was one of the major components that formed on the steel surface as revealed in spectrum b) by the vibration bands at 283 cm^{-1} and 1085 cm^{-1} [17]. The formation of such a calcareous deposit was expected and was due to the increase of the interfacial pH associated with CP.

IV. Conclusions

Voltammetry was used successfully to study the behavior of carbon steel coupons buried in an artificial soil wetted at 65-70% saturation:

- Depending on the local soil environment, the corrosion rate at OCP was measured between 160 µm/y (coupon CP2 at day 7) and 300 µm/y (coupon WE at day 37). These values were consistent with previous work [7] and the difference observed between the coupons was mainly due to changes of the active area. The active area depended on the local moisture level of the soil.
- Via the modeling of the voltammograms acquired at the end of the experiment with coupons subjected to CP for 30 days it proved possible to quantify the direct and induced effects of CP. The direct effect resulted from decreased potential. When the potential was decreased from -0.775 V to -0.834 V, the corrosion rate reduced from 25 µm/y to 12 µm/y. The second effect was the indirect effect induced by CP, i.e., the formation of a protective layer due to the increased interfacial pH. This effect led to decreased τ_{cor} from 160 µm/y to 25 µm/y between day 7 and day 37.

Acknowledgments

This study is part of the collaborative Ph.D. study at the University of Johannesburg and the University of La Rochelle, carried out by Mandlenkosi G.R. Mahlobo and financially supported by the National Research Foundation (NRF) - South Africa.

References

[1] William, S.F. and Javad, H. (2006), Foundations of Materials Science and Engineering (4th ed.), McGraw-Hill, ISBN 0-07-295358- 6
[2] Ismail, A.I.M. and El-Shamy, A.M. (2009). "Engineering behavior of soil materials on the corrosion of mild steel." Applied Clay Science 42: 356-362.
[3] Yan, M., Sun, C., Xu, J., Dong, J. and Ke, W. (2014). "Role of Fe oxides in corrosion of pipeline steel in a red clay soil." Corrosion Science 80: 309-317.
[4] Kodym, R., Snita, D., Fíla, V., Bouzek, K. and Kouri, M. (2017a). "Investigation of processes occurring at cathodically protected underground installations: Experimental study of pH alteration and mathematical modeling of oxygen transport in soil." Corrosion Science 120: 14-27.
[5] Kodym, R., Snita, D., Fíla, V., Bouzek, K. and Kouril, M. (2017b). "Investigation of processes occurring at cathodically protected underground installations: Mathematical modeling of reaction-transport processes in soil." Corrosion Science 120: 28-41.
[6] Cole, I.S. and Marney, D. (2012). "The science of pipe corrosion: A review of the literature on the corrosion of ferrous metals in soils." Corrosion Science 56: 5-16.
[7] Akkouche, R., Rémazeilles, C., Jeannin, M., Barbalat, M., Sabot, R. and Refait, Ph. (2016). "Influence of soil moisture on the corrosion processes of carbon steel in artificial soil: Active area and differential aeration cells." Electrochimica Acta 213: 698-708.
[8] Nguyen, D.D., Lanarde, L., Jeannin, M., Sabot, R. and Refait, Ph. (2015). "Influence of soil moisture on the residual corrosion rates of buried carbon steel structures under cathodic protection." Electrochimica Acta 176: 1410-1419.
[9] Barbalat, M., Lanarde, L., Caron, D., Meyer, M., Vittonato, J., Castillon, F., Fontaine, S. and Refait, Ph. (2012). "Electrochemical determination of residual corrosion rates of steel under cathodic protection in soils." Corrosion Science 55: 246-253.
[10] Barbalat, M., Caron, D., Lanarde, L., Meyer, M., Fontaine, S., Castillon, F., Vittonato, J. and Refait, Ph. (2013). "Estimation of residual corrosion rates of steel under cathodic protection in soils via voltammetry." Corrosion Science 73: 222-229.
[11] Akkouche, R., Rémazeilles, C., Barbalat, M., Sabot, R., Jeannin, M. and Refait, Ph. (2017). "Electrochemical monitoring of steel/soil interfaces during wet/dry cycles." Journal of Electrochemical Society 164(12): 626-634.
[12] Rahal, C., Masmoudi, M., Abdelhedi, R., Sabot, R., Jeannin, M., Bouaziz, M. and Refait, Ph. (2016). "Olive leaf extract as a natural corrosion inhibitor for pure copper in 0.5M NaCl solution: A study by voltammetry around OCP" Journal of Electroanalytical Chemistry 769: 53-61.
[13] Gupta, S.K. and Gupta, B.K. (1979). "The critical soil moisture content in the underground corrosion of mild steel" Corrosion Science 19. 171-178.
[14] Neale, C.N., Hughes, J.B. and Ward, C.H. (2000). "Impacts of unsaturated zone properties on oxygen transport and aquifer reaeration" Ground Water 38. 784–794.
[15] Leeds, S.S. and Cottis, R.A. (2006). "An investigation into the influence of surface films on the mechanism of cathodic protection",

CORROSION/2006, paper No. 06084, National Association of Corrosion Engineers, Houston, Texas.
[16] De Faria, D.L.A., Silva, S.V. and Oliveira, M.T.D. (1997). "Raman micro spectroscopy study of some iron oxides and oxyhydroxides" J. Raman Spectroscopy. 28. 873–878.
[17] Tomic, Z. Makreski, P. and Gajic, B. (2010). "Identification and spectra–structure determination of soil minerals: Raman study supported by IR spectroscopy and X-ray powder diffraction" J. Raman Spectroscopy. 41. 582-586.